Performance modelling and greenhouse impact assessment of a micro-ORC energy system working with HFCs, low GWP fluids and mixtures

Michele Bianchi[1], *Lisa* Branchini[1], *Andrea* De Pascale[1], *Francesco* Melino[1], *Saverio* Ottaviano[1], *Antonio* Peretto[1] and *Noemi* Torricelli[1*]

[1]Università di Bologna – DIN, Viale del Risorgimento 2, 40136 Bologna, Italia

Abstract. The worrying effects of climate change have led, in the last decades, to the improvement of innovative solutions for low greenhouse emission energy conversion, among which, is the use of micro-ORC (Organic Rankine Cycle) systems for distributed generation, in the framework of combined heat and power applications and renewables exploitation. However, micro-ORCs environmental impact, due to high GWP (global working potential) working fluid leak rate, is an issue still to overcome. Neverthless the interest in using new low GWP refrigerants and their blends is increasing, new fluids have not yet been properly tested into ORC. Numerical studies reveal that low GWP fluids do not always guarantee the same performance of typically used fluids, leading to indirect emissions related to the use of fossil fuels to compensate the lower power production. This study proposes to investigate performance and impact of an innovative micro-ORC test bench when working with HFCs (HydroFluoroCarbons), low GWP fluids and mixtures, with the main aim of comprehensively evaluating its impact due to both direct and indirect greenhouse gas emissions produced in a typical annual operation.

1 Introduction

Experts agree that main potential solutions to achieve reduction of greenhouse emissions rely on: the improvement in the systems conversion efficiency, the increase of renewables in the energy mix and the on-site generation of electricity. In particular, power generation from low-grade heat sources (i.e. below 200 °C) is gaining interest as method to implement the aforementioned solutions. In this context, the Organic Rankine Cycle (ORC) is one of the most suitable technologies for valorising low-grade heat into electricity or mechanical power [1].

The selection of the working fluid for an ORC represents a key decision, affecting the system design and the related performance. In particular, most common fluids employed for low-temperature applications are refrigerants belonging to HydroFluoroCarbons (HFCs) category [2]. Refrigerants appear to be very performing for these applications thank to their low critical temperature. On the other hand, HFCs risk to highly contributing to the greenhouse effect, if released, due to their high global warming potential (GWP) values and high residence time in the atmosphere. Possible modern substitutes of HFCs, have been identified in the HydroFluoroOlefines (HFOs), which presents similar properties to HFCs but very lower GWP values [3]. Although HFOs have been already widely tested in refrigeration plants, properly test for ORC applications are limited. Some numerical studies have been conducted revealing that low GWP fluids could not always guarantee the same performance of commonly used fluids [4].

In view of the above, this study intends to explore the actual greenhouse impact of micro-ORC systems, which derives from the use of low-GWP fluids, in place of HFCs, and vice versa. Authors propose a comprehensive evaluation, which accounts not only for direct greenhouse emissions, due to refrigerant leakage during the system operation, but also for indirect contribute. Indirect emissions are defined as those emissions related to the use of fossil fuels to generate the lack of power production caused by the use of a less performing fluid over a more performing one.

This analysis, in particular, takes as a reference a micro-ORC system presented in [5]. The reference system [5] consists of a kW scale recuperated ORC conceived for heat source temperature below 100 °C.

* Corresponding author: noemi.torricelli2@unibo.it

The key component of the system is the expander, a prototype of reciprocating model. The expander is directly coupled with the generator, which is connected to an electrical load, made of five pure resistive loads. The feed pump is an external gear type, driven by an asynchronous electric motor. The pump motor is driven by a frequency inverter, which allows a proper regulation of the flow rate of the working fluid, since the pump is of positive displacement type.

The first step consists in assessing the micro-ORC performance. The second step comprises the simulation of the plant behaviour over a typical annual operation, to determine the yearly energy production and corresponding greenhouse emissions. More in detail, the examined operating conditions refer to an existing micro-ORC operation, installed at a pool centre [6]. The system is conceived to exploit a geothermal liquid-dominated well hot source, while the cold sink is the swimming pool heating circuit.

2 Methodology

2.1 Micro-ORC performance model

A schematic of the system model, describing the components sub-models and relationships between them, is shown in Fig. 1. The inputs of the model are the control variables and the boundary conditions of the system. Six main parameters can be controlled from the outside: the hot source temperature and flow rate at the evaporator inlet, T_{H2Ohot} and $\dot{m}_{H2Ohot}$, cold source temperature and flow rate at the condenser inlet, $T_{H2Ocold}$ and $\dot{m}_{H2Ocold}$, feed pump frequency, f_{pp}, and number of resistive loads activated, n_{loads}. Plus, the subcooling level at the condenser outlet, ΔT_{sc}, which depend on the fluid charge, the cold source temperature and the non-condensable gas content [7]. Since the ORC model is formulated as an implicit problem, its solution is determined through an iterative process, whose iterative variables are the condensing pressure (p_{cd}) and the expander inlet temperature (T_1). The outputs variables are the fluid states in all the point of the thermodynamic cycle. Four additional indicators, namely, the thermal input provided at the evaporator, $\dot{Q}_{ev}$, the condenser discharged heat, $\dot{Q}_{cd}$, the electric power output, $\dot{W}_{exp}$, and the pump absorbed power, $\dot{W}_{pp}$ have been included as model output variables.

The considered sub-models are the pump and the circuit resistance, the expander, the recuperator, the evaporator and the condenser ones (respectively indicated by the "PP & RES", "EXP", "REC", "EV" and "CD" blocks in Fig. 1). Semi-empirical model approach is chosen for each component rather than constant-efficiency one, as more accurate in simulating the performance of ORC systems, with robust prediction in both fitting and extrapolation [8]. In this study, experimental data collected during the reference rig experimental tests [5] using R134a have been considered for the calibration. Sub-models and their empirical parameters requiring calibration are listed in Tab. 1. It must be highlighted that some empirical parameters are associated only to the components dimensions whilst others depend on the working fluid thermodynamic characteristics. For this reason, parameters related to the working fluid will be corrected to account for the use of fluids different from R134a.

Tab. 1. Model parameters.

Sub-model	Parameters
EV, CD, REC	$\alpha_{wf,ref}$, $\dot{m}_{wf,ref}$, $\Delta T_{sat,ref}$, x, y, A
EXP	$(AU)_{su,ref}$, $(AU)_{ex,ref}$, $(AU)_{amb}$, $r_{v,exp}$, $r_{v,comp}$, V_0, A_{leak}, A_{su} $W_{loss,ref}$, $W_{loss,N}$ [10]
PP & RES	c_1, c_2, c_3, c_4, η

The model as a whole has been implemented in the Matlab environment; the thermodynamic properties of the fluids have been calculated by means of the REFPROP library.

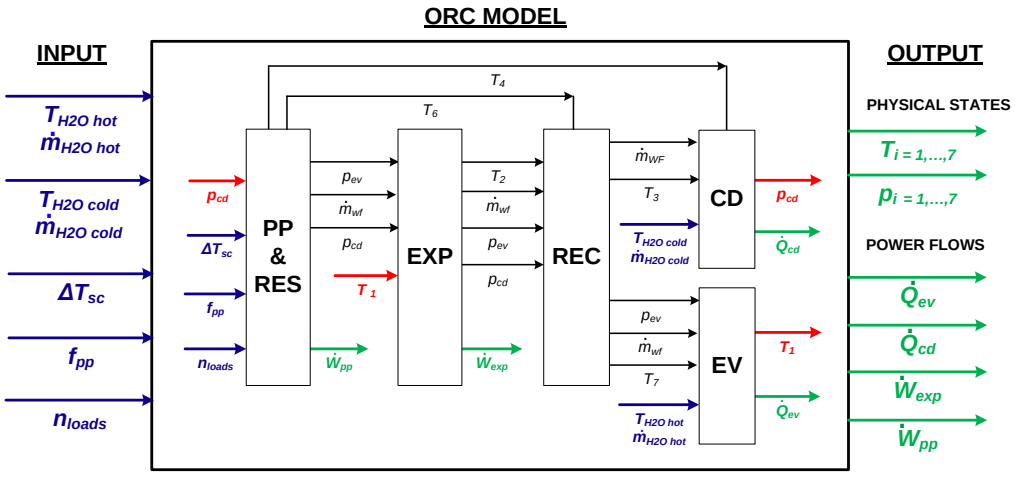

Fig. 1. Schematic of the cycle model (inputs of the model are indicated in blue, iterative variables in red, intermediate variables in black and outputs of the model in green).

2.1.1 Heat exchangers

Performance of evaporator and the condenser are obtained by means of a three-zone lumped parameters moving boundary model with variable heat transfer coefficients. According to this approach, the heat exchanger is decomposed into three different heat exchange regions (namely: Subcooled, TP - Two Phase and Superheated), the boundaries of which are defined by the thermodynamic phase change points of the working fluid. Each zone is characterized by a global heat transfer coefficient U_i and a heat transfer surface area A_i. The sum of the single surface areas corresponds to the geometrical surface area of the component, A, which is a model parameter. The heat transfer occurring in the *i-th* zone is given by the product between the global heat transfer coefficient, the surface area and the logarithmic mean temperature difference $\Delta T_{log,i}$ (Eq. (1)).

$$\dot{Q}_i = A_i U_i \cdot \Delta T_{log,i} \tag{1}$$

The considered global heat transfer coefficient accounts for the convective coefficient of the working fluid side, α_{wf}, and the convective coefficient of the water side. Dittus-Boelter correlation for forced convection is used to evaluate the water convective coefficients and the working fluid convective coefficients for the subcooling and the superheating zone. The working fluid convective coefficient for the two-phase zone, $\alpha_{wf,TP}$, derives instead from empirical correlations. In particular, correlation used for the evaporator has the form of Eq. (2).

$$\alpha_{wf,TP} = \alpha_{wf,TP,ref} \left(\frac{\dot{m}_{wf}}{\dot{m}_{wf,ref}} \right)^x \left(\frac{\Delta T_{sat}}{\Delta T_{sat,ref}} \right)^y \tag{2}$$

where $\alpha_{wf,ref}$ represents the value of the convective coefficient in reference operating conditions. $\alpha_{wf,ref}$ is adjusted as function of two terms of influence: i) the working fluid mass flow rate, $\dot{m}_{wf}$; ii) the difference between the working fluid saturation temperature and the water temperature, ΔT_{sat}. In this way, $\alpha_{wf,TP}$ accounts for the dependence of the convective coefficient from both the fluid velocity, and the nucleated boiling convection contribute, which is proportional to ΔT_{sat} [9]. Correlation used for the condenser is the same of Eq. (2), but assuming pure convective regime, thus, excluding the dependence from ΔT_{sat}. The recuperator is also modelled on the basis of Eq. (1), but considering a single heat exchange zone.

2.1.2 Reciprocating piston expander

The volumetric expander is simulated by means of the grey-box model, validated for the reference reciprocating expander in a previous work of the Authors [10]. The model follows a lumped parameters approach as illustrated by the scheme shown in Fig. 2. Equations of the model describe the internal expansion, the re-compression phenomena and additional characteristic power losses, such as under/over-expansion losses, pressure losses, internal leakages, heat dissipation, frictions and electro-mechanical conversion losses. The reader is invited to refer to [10] for a detailed description of the expander model. In this analysis the built-in volume ratio value is chosen equal to its optimum, which allows to obtain the maximum expander power output, as demonstrated in [4].

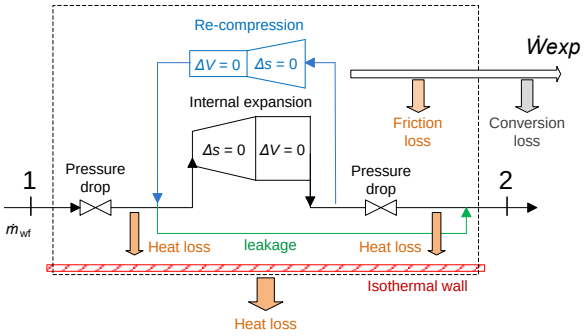

Fig. 2. Schematic of the expander model

2.1.3 Pump and circuit resistance

According to the method proposed by the Authors [4], the pump operating point is determined by crossing the pump characteristic curve for a given rotational speed and the resistance characteristic of the circuit in which the pump is inserted. Extrapolated curves of the gear pump in exam [4] are shown in Fig. 3 in terms of pressure rise versus volumetric flow rate. The "Frequency" curves represent the pump performance at different rotating speed, whilst the "Loads" curves represent the circuit resistance. Indeed, the number of the activated resistive loads dissipating the electric power output influences the actual resistance of the system.

The mass flow rate, output of the "PP & RES" sub-model is obtained as function of the volumetric flow rate, using the fluid density at the pump inlet. The product between the pressure rise, Δp, and the volumetric flow rate, $\dot{V}$, divided by the pump efficiency, η, gives the pump absorbed power (Eq. (3)).

$$\dot{W}_{pp} = \frac{\dot{V} \cdot \Delta p}{\eta} \tag{3}$$

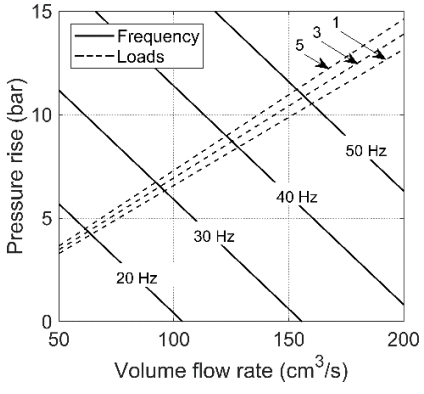

Fig. 3. Gear pump and circuit resistance characteristics.

2.1.4 Correction of fluid dependent parameters

The global heat transfer coefficients have been re-determined adopting the procedure proposed by Giuffrida [11] to account for fluid replacement. The global heat transfer coefficient can be evaluated as:

$$U = \frac{Nu \cdot \lambda}{L} \tag{4}$$

where Nu and λ are the Nusselt number and the conductivity, which depend on the fluid thermodynamic properties; whilst L is the characteristic length and it is set by the component geometry. Thus, the global heat transfer coefficient for the new fluid, U_{new}, can be determined as function of the reference global heat transfer coefficient, U_{ref}, and the fluids properties, by using Eq. (5).

$$\frac{U_{new}}{U_{ref}} = \frac{Nu_{new} \cdot \lambda_{new}}{Nu_{ref} \cdot \lambda_{ref}} \tag{5}$$

Concerning the pump and circuit resistance model, according to [4], the change of the fluid induces a change in the pump and circuit resistance curves slope (curves shown in Fig. 3) as resumed below. Eq. (6) and Eq. (7) are the base equations describing respectively the pump and the circuit resistance curves. In particular, according to Eq. (6), the volumetric flow rate elaborated by the pump, $\dot{V}$, is the difference between the theoretical volumetric flow rate, $\dot{V}_{th}$, and the leakage one, $\dot{V}_{leak}$, lost through the meatus. $\dot{V}_{th}$ depends on the pump geometry and rotational speed, while $\dot{V}_{leak}$ can be calculated as a function of geometrical data, operating pressure and fluid viscosity by means of Poiseuille's law.

$$\dot{V} = \dot{V}_{th}(geo_{pp}, N_{pp}) - \dot{V}_{leak}(geo_{pp}, \Delta p, \mu) \tag{6}$$

Eq. (7) represents the general formula for evaluating hydraulic circuit pressure head, Δp, where ε, is the equivalent flow coefficient, ρ, is the fluid density and w, the fluid velocity.

$$\Delta p = \varepsilon(geo_{circ}, n_{loads}) \cdot \rho \cdot \frac{w^2(geo_{circ}, \dot{V}, \rho)}{2} \tag{7}$$

Eqs. (6) and (7) can be rearranged by expliciting the terms indicated in brackets, highlighting the relationship between ΔP, $\dot{V}$, N_{pp} and n_{loads}

$$\Delta p = (c_1 \cdot N_{pp} + c_2 \cdot \dot{V}) \cdot \mu \tag{8}$$

$$\Delta p = (c_3 \cdot n_{loads} + c_4) \cdot \dot{V} \cdot \rho \tag{9}$$

where c_1, c_2, c_3 and c_4 are constants that contain the pump and the circuit geometry (geo_{pp}, geo_{circ}). Thus, the only terms related to the working fluid remain the fluid density, ρ, and the fluid viscosity, μ, influencing the characteristic curves slope.

2.2 Micro-ORC environmental impact assessment

The total GHG emissions from an ORC system can be estimated by taking into account two main terms, namely direct emissions and indirect emissions. Direct emissions, Em_{direct}, include the environmental impact of leakage of refrigerant, which occurs during system operation and servicing, and can be expressed as:

$$Em_{direct} = m \cdot LR \cdot GWP \tag{10}$$

where m is the system's fluid charge, LR, the annual leak rate and, GWP, global warming potential of the working fluid. The fluid charge is estimated on the basis of the internal volume of the largest ORC components, i.e. the evaporator, the condenser, the recuperator and the liquid receiver. The fluid mass enclosed in the j-th component could be estimated as the product between the *j-th* component volume and the *j-th* mean fluid density [12].

Indirect GHG emissions are also considered in this study to compare fluids. The aim is to account for the potential CO_2 emissions related to the use of fossil fuels to compensate the energy production gap due to a less performing fluid over a more performing one. Indeed, the ORC can operate with different conversion efficiency when working with different fluids. This leads to different yearly energy production, for a given heat source thermal input profile. In order to perform a fair comparison, the energy gap (E_{gap}) caused using a less performing fluid must be filled with energy sources outside the ORC system, likely employing conventional fuels. Thus, indirect emissions ($Em_{indirect}$) results by the product between the energy gap, E_{gap}, and the emission factor, β, of the substitute energy provider:

$$Em_{indirect} = E_{gap} \cdot \beta \tag{11}$$

where E_{gap} is given by the difference between the energy produced by using the most performant fluid (E_{max}) and the energy produced by using the fluid in exam (E).

$$E_{gap} = E_{max} - E \tag{12}$$

With the aim of evaluating the ORC annual operation, all the energy terms are calculated on the yearly basis. In this case, β is assumed equal to 460 $kgCO_2/MWh$, which corresponds to the EU-27 emission factor for electricity consumed, provided by EU 2017 technical report about default emission factors [13].

3 Tested conditions and results

In order to determine the final energy production and GHG emissions of the system, a yearly operating cycle can be taken into account. The case study of a real geothermal application at a swimming pool centre [6] has been investigated in this study. On the basis of this, the following boundary conditions are imposed to investigate the ORC representative working point:

- T_{H2Ohot} = 60°C; $\dot{m}_{H2Ohot}$ = 22 m³/h;
- $T_{H2Ocold}$ = 18°C; $\dot{m}_{H2Ocold}$ = 25 m³/h;
- f_{pp} = adjusted to reach the evaporating pressure that leads to the best ORC net power output for each working fluid (a minimum superheating degree of 3 °C is imposed as constraint)
- ΔT_{sc}= 4 ° C, according to observed experimental values [5].
- n_{loads} = 5, corresponding to an electric power of 3 kW.

Fluids analysed in this work are: i) R134a; ii) its low GWP alternatives R1234yf and R1234ze(E); iii) a mixture of 50% R134a and 50 % R1234yf, and a mixture of 50 % R134a and 50 % of R1234ze(E). R1234yf and R1234ze(E) are chosen among HFOs commercially available fluids, as most suitable for heat recovery applications at temperature lower than 100 °C (given their critical temperature close to 100 °C).

3.1 Results

Emissions related to the ORC operation during the representative year are examined and compared among analysed fluids.

Indirect and direct greenhouse gas (GHG) emissions are affected by performance output (listed in Tab. 2) namely:

- the yearly electric energy gap, which must be provided by external fossil fuel sources (Eq (11));
- the system fluid charge and leak rate (see Eq. (12)).

Results show that R134a presents the highest yearly net electric energy production (9621 kWh) followed by the blends, with a decrease of about 17 %, and then by R1234yf and R1234ze(E), with an additional decrease of almost 19 %. For this reason, R134a yearly energy production has been considered as reference (E_{max}), when applying Eq. (18). The highest E_{gap} value is calculated in case of R134ze(E). Main factors determining the performance drop introduced using HFO fluids can be identified in: (i) the lower pressure ratio (leading to smaller enthalpy drop available through the expander); (ii) the lower viscosity (mainly affecting the leakage losses at the pump meatus and thus the elaborated mass flow rate, for more detail refer to [4]). The overall performance obtained with mixtures are intermediate between the performance of the pure fluids.

The leak rate is assumed equal to 2 % as characteristic value provided for Residential and Commercial A/C, including Heat Pumps, by IPCC Good Practice Guidelines and Uncertainty Management in National Greenhouse Gas Inventories (2000) [14]. Since specific data for ORC are scarce and not available, for sake of completeness, a parametric analysis by varying the leak rate is also proposed.

Results of the greenhouse impact assessment are presented in terms of specific emissions per unit of produced energy (E). Surprisingly, concerning total emissions, Fig. 4 reveals that HFOs do not reduce total CO_2 equivalent emissions, even if they reduce the direct contribution. Actually, using R1234yf increases total specific emission by 126 % and using R1234ze(E) even by 181 %. Blends instead exhibits intermediate emissions compared to pure fluids forming the mixture. Total emissions related to the use of R134a are associated to only direct emissions. Conversely, total emissions related to the use of HFOs are basically equal to only indirect emissions since the direct emissions contribution (of about 0.4 $kgCO_2$/MWh) is negligible compared to indirect contribute.

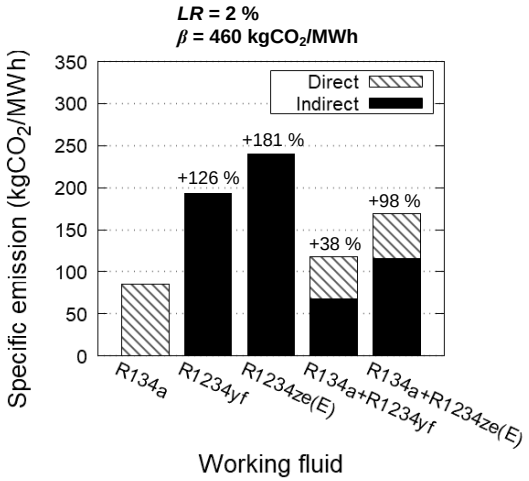

Fig. 4. CO_2 equivalent emissions – fluids comparison (percentage related to R134a total emissions).

Parametric analysis demonstrates that emissions are quite sensitive to the leak rate and the energy mix emission factor. Higher leak rate, indeed, scale up direct emission, giving greater importance to direct contribution. Values of the leak rate up to 15 % have been explored, where 17 % is the typical annual leak rate associated to Centralised Supermarket Refrigeration Systems [14]. A parametric analysis has been added also to explore the influence of emission factor [13] (Fig. 6). It must be noticed that higher emissions factors lead to higher indirect emissions and could discourage the use of low GWP as alternatives of R134a. Anyway, with a view to move towards a greener energy mix, emissions factors are expected to decrease in next years and the use of low GWP fluids will probably help to effectively reduce GHG emissions.

Tab. 2. ORC performance affecting GHG emissions – fluids comparison.

Parameters \Fluids	**R134a**	**R1234yf**	**R1234ze(E)**	**R134a + R1234yf**	**R134a + R1234ze(E)**
Yearly net electric energy, E (kWh)	9621 (=E_{max})	6777	6323	8378	7684
Yearly electric energy gap, E_{gap} (kWh)	0	2843	3298	1243	1937
Working fluid charge, m (kg)	28.8	27.4	27.1	28.9	28.5

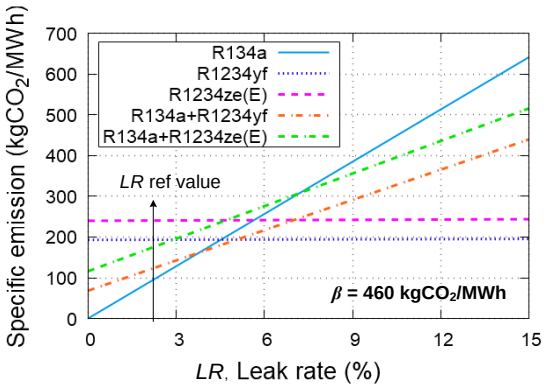

Fig. 5. CO_2 equivalent emissions as function of the leak rate – fluids comparison.

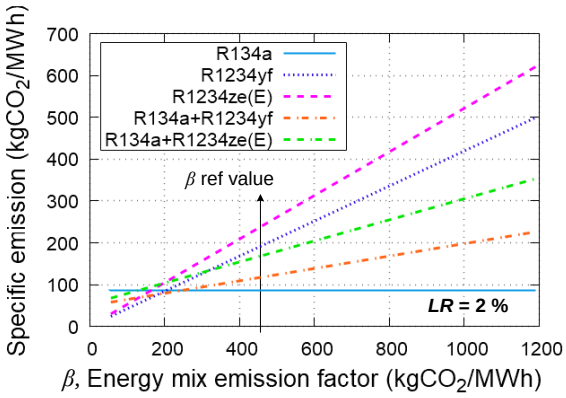

Fig. 6. CO_2 equivalent emissions as function of the energy mix emission factor – fluids comparison.

4 Conclusion

A methodology to account for direct and indirect greenhouse gas emissions contributes is proposed to evaluate R134a replacement with low GWP fluids in a micro-ORC system.

The performed analysis reveals that HFO fluids cannot always guarantee the same performance of R134a, even if they exhibit very lower GWP. Thus, HFOs introduce an energy production gap, which can be compensated with external energy sources, like fossil fuels. If considering a leak rate equal to 2%, indirect emissions caused using HFOs determine total equivalent emissions of CO_2 greater than the ones related to R134a, up to + 181 %. A parametric study by varying the leak rate value highlights that emissions are quite sensitive to this parameter. Thus, knowing the actual annual leak rate of the system is important in order to perform a correct evaluation of the greenhouse impact. Other factor of influence is the emission factor of the energy mix considered to provide the energy production gap. It must be noticed, indeed, that higher emissions factors lead to higher indirect emissions and could discourage the use of low GWP as alternatives of R134a. Anyway, recent energy targets intend to push toward greener energy mix, emissions factors are expected to decrease and the use of low GWP fluids may help to effectively reduce greenhouse gas emissions. At least, in this transition period, blends could help to maintain a good trade-off between performance and greenhouse impact.

References

1. Tocci, L. et Al. Small Scale Organic Rankine Cycle (ORC): A Techno-Economic Review. *Energies* **2017**, *10*.
2. Park, B. et Al. Review of Organic Rankine Cycle experimental data trends. *Energy Convers. Manag.* **2018**, *173*, 679–6917.
3. Heredia-Aricapa, Y. et Al. Overview of low GWP mixtures for the replacement of HFC refrigerants: R134a, R404A and R410A. *Int. J. Refrig.* **2020**, *111*.
4. Ancona, M. A. et Al. Performance prediction and design optimization of a kW-size reciprocating piston expander working with low-GWP fluids. In Proceedings of the 5th International Seminar on ORC Power Systems; Athens, Greece, 2019.
5. Bianchi, M. et Al. Experimental analysis of a micro-ORC driven by piston expander for low-grade heat recovery. *Appl. Therm. Eng.* **2019**, *148*, 1278–1291.
6. Bianchi, M. et Al. Performance and operation of micro-ORC energy system using geothermal heat source. *Energy Procedia* **2018**, *148*, 384–391.
7. Ziviani, D. et Al. Effects of the Working Fluid Charge in Organic Rankine Cycle Power Systems: Numerical and Experimental Analyses. *Org. Rank. Cycle Technol. Heat Recovery* **2018**.
8. Dickes, R. et Al. Modelling of organic Rankine cycle power systems in off-design conditions: An experimentally-validated comparative study. *Energy* **2017**, *123*, 710–727.
9. *A-to-Z Guide to Thermodynamics, Heat and Mass Transfer, and Fluids Engineering: AtoZ*; Begellhouse, 2006; Vol. F.
10. Bianchi, M. et Al. Application and comparison of semi-empirical models for performance prediction of a kW-size reciprocating piston expander. *Appl. Energy* **2019**, *249*, 143–156.
11. Giuffrida, A. Modelling the performance of a scroll expander for small organic Rankine cycles when changing the working fluid. *Appl. Therm. Eng.* **2014**, *70*, 1040–1049.
12. Liu, L. et Al. Working fluid charge oriented off-design modeling of a small scale Organic Rankine Cycle system. *Energy Convers. Manag.* **2017**, *148*.
13. Cerutti, A.K. et Al. Joint Research Centre *Covenant of Mayors for Climate and Energy: default emission factors for local emission inventories : version 2017.*; 2017.
14. Accuvio leakage rate (%) for the refrigeration/air-con/HVAC Available online: https://support.accuvio.com/support/solutions/articles/4000040366-annual-leakage-rate-for-the-refrigeration-air-con-hvac-